2014年度 計測自動制御学会四国支部学術講演会

講演論文集

SICE SHIKOKU JAPAN

会　場:愛媛大学 総合情報メディアセンター
会　期:2014 年 11 月 28 日(金)
28 November 2014

主 催:公益社団法人 計測自動制御学会 四国支部

御挨拶

計測自動制御学会四国支部学術講演会2014は，「計測」と「自動制御」をキーワードとして，企業，大学，高専，などの研究者および技術者が一堂に会し，その研究や技術を紹介し，討論と情報交換を行うことによって四国における計測・自動制御分野の研究の活性化を図ることを目的としています．特に若手の企業の研究者・技術者にこのような場を提供し，一層飛躍する機会になればと思います．本講演会は毎年１回開催されており，今年で第７回になります．ショートオーラルセッション（概要を短時間で口頭発する）およびポスターセッション（参加者と対面して自由に議論する）を行うハイブリット講演にて構成され，講演者と聴講者がより有意義な議論を交わしていただけるものと期待しています．なお，若手研究者による優秀な発表には優秀講演賞を授与します．また，特別講演としましては，画像処理分野で著名な土井章男先生（岩手県立大学教授）をお招きしまして，「X線CTと3Dプリンタによる造形技術と医療分野への応用」と言う演

SO2-11, PS2-11

Development and Vibration Control of a Flexible Single-link Manipulator Using a Piezoelectric Actuator

Abdul Kadir Muhammad[1,2], Shingo Okamoto[1], and Jae Hoon Lee[1]

[1]Graduate School of Science and Engineering, Ehime University, Japan
(Tel: 81-97-594-0181, Fax: 81-97-594-0181)

[2]Center for Mechatronics and Control Systems, Department of Mechanical Engineering,
State Polytechnic of Ujung Pandang, Indonesia

[1]y861008b@mails.cc.ehime-u.ac.jp

Abstract

The purposes of this research are to formulate the equations of motion of the system, to develop computational codes by a finite-element method in order to perform dynamics simulation with vibration control, to propose an effective control scheme using two control strategies, namely proportional (P) and active-force (AF) controls and to confirm the calculated results by experiments of a flexible link manipulator. The system used in this paper consists of an aluminum beam as a flexible link, a clamp-part, a servo motor to rotate the link and a piezoelectric actuator to control vibration. Computational codes on time history responses, FFT (Fast Fourier Transform) processing and eigenvalues - eigenvectors analysis were developed to calculate the dynamic behavior of the link. Furthermore, the P and AF controls strategies were designed and compared their performances through calculations and experiments. The calculated and experimental results showed the superiority of the proposed AF control compared to the P one to suppress the vibration of the flexible link manipulator.

1 INTRODUCTION

Employment of flexible link manipulator is recommended in the space and industrial applications in order to accomplish high performance requirements such as high-speed besides safe operation, increasing of positioning accuracy and lower energy consumption, namely less weight. However, it is not usually easy to control a flexible manipulator because of its inheriting flexibility. Deformation of the flexible manipulator when it is operated must be considered by any control. Its controller system should be dealt with not only its motion but also vibration due to the flexibility of the link.

The purposes of this research are to derive the equations of motion of a flexible single-link system by a finite-element method, to develop the computational codes in order to perform dynamics simulations with vibration control, to propose an effective control scheme of a flexible single-link manipulator using two control strategies, namely proportional (P) and active-force (AF) controls and to confirm the calculated results by experiments of the flexible link manipulator.

The flexible manipulator used in this paper consists of an aluminum beam as a flexible link, a clamp-part, a servo motor to rotate the link and a piezoelectric actuator to control vibration. Computational codes on time history responses, FFT (Fast Fourier Transform) processing and eigenvalues - eigenvectors analysis were developed to calculate the dynamic behavior of the link and validated by the experimental one. Furthermore, the P and AF controls strategies were designed to suppress the vibration. It was done by adding bending moments generated by the piezoelectric actuator to the single-link. Finally, their performances were compared through calculations and experiments.

2 FORMULATION BY FINITE-ELEMENT METHOD

The link has been discretized by finite-elements [1] - [4]. The finite-element has two degrees of freedom, namely the lateral deformation $v(x,t)$, and the rotational angle $\psi(x,t)$. The length, the cross-sectional area and the area moment of inertia around z-axis of every element are denoted by l_i, S_i and I_{zi} respectively. Mechanical properties of every element are denoted as Young's modulus E_i and mass density ρ_i.

2.1 Kinematics

Fig. 1 shows the position vector $\boldsymbol{r}$ of an arbitrary point P in the link in the global and rotating coordinate frames. Let the link as a flexible beam has a motion that is confined in the horizontal plane as shown in figure 1. The $O - XY$ frame is the global coordinate frame while $O - xy$ is the rotating coordinate frame fixed to the root of the link. The unit vectors in X, Y, x and y axes are denoted by $\boldsymbol{I}$, $\boldsymbol{J}$, $\boldsymbol{i}$ and $\boldsymbol{j}$, respectively. A motor is installed on the root of the link. The rotational angle of the motor when the link rotates is denoted by $\theta(t)$.

The position vector $\boldsymbol{r}(x,t)$ of the arbitrary point P in the link at time $t = t$, measured in the $O - XY$ frame shown in figure 1 is expressed by

$$\boldsymbol{r}(x,t) = X(x,t)\boldsymbol{I} + Y(x,t)\boldsymbol{J} \tag{1}$$

Where

$$X(x,t) = x\cos\theta(t) - v(t)\sin\theta(t) \tag{2}$$
$$Y(x,t) = x\sin\theta(t) + v(t)\cos\theta(t) \tag{3}$$

The velocity vector of P at time $t = t$ is given by

$$\dot{\boldsymbol{r}}(x,t) = \dot{X}(x,t)\boldsymbol{I} + \dot{Y}(x,t)\boldsymbol{J} \tag{4}$$

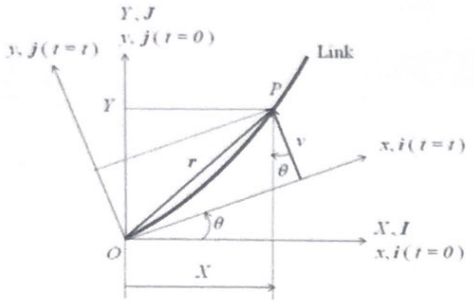

$O-XY$: Global coordinate frame
$O-xy$: Rotating coordinate frame

Fig.1. Position vector of an arbitrary point P in the link in the global and rotating coordinate frames

2.2 Equations of motion

Equation of motion of the *i-th* element is given by

$$\boldsymbol{M}_i\ddot{\boldsymbol{\delta}}_i + \boldsymbol{C}_i\dot{\boldsymbol{\delta}}_i + \left[\boldsymbol{K}_i - \dot{\theta}^2(t)\boldsymbol{M}_i\right]\boldsymbol{\delta}_i = \ddot{\theta}(t)\boldsymbol{f}_i \tag{5}$$

where $\boldsymbol{M}_i$, $\boldsymbol{C}_i$, $\boldsymbol{K}_i$, $\ddot{\theta}(t)\boldsymbol{f}_i$ are the mass matrix, damping matrix, stiffness matrix and the excitation force generated by the rotation of the motor respectively. The representation of the matrices and vector in Eq. (5) can be found in [1] and [3]. Finally, the equation of motion of the system with n elements considering the boundary conditions is given by

$$\boldsymbol{M}_n\ddot{\boldsymbol{\delta}}_n + \boldsymbol{C}_n\dot{\boldsymbol{\delta}}_n + \left[\boldsymbol{K}_n - \dot{\theta}^2(t)\boldsymbol{M}_n\right]\boldsymbol{\delta}_n = \ddot{\theta}(t)\boldsymbol{f}_n \tag{6}$$

3 MODELING

Fig. 2 shows a model of the single-link manipulator, the clamp-part and the piezoelectric actuator. The link including the clamp-part and actuator were discretized by 35 elements. The clamp-part is more rigid than the link. Therefore Young's modulus of the clamp-part was set in 1,000 times of the link's. The piezoelectric actuator was bonded to a one-side surface of Element 4. A schematic representation on modeling of the piezoelectric actuator is shown in Fig. 5. Furthermore, a strain gage was bonded to the position of Node 6 of the single-link (0.11 m from the origin). Physical parameters of the single-link model and the piezoelectric actuator are shown in table 1 [2].

The piezoelectric actuator suppressed the vibration of the flexible link manipulator by adding bending moments at Nodes 3 and 6, M_3 and M_6 to the flexible link. The bending moments are generated by applying voltages E to the piezoelectric actuator as shown in Fig. 3. The relation between the bending moments and the voltages are related by

$$M_3 = -M_6 = d_1 E \tag{7}$$

Here d_1 is a constant quantity.

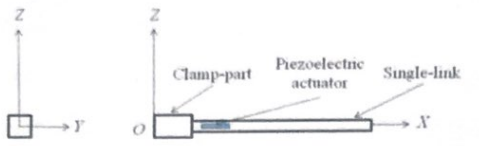

Fig.2. Computational models of the flexible single-link manipulator

Tabel.1 Physical parameters of the single-link model and the piezoelectric actuators

l : Total length	m	3.91×10^{-1}
l_l : Length of the link	m	3.50×10^{-1}
l_c : Length of the clamp-part	m	4.10×10^{-2}
l_a : Length of the actuator	m	2.00×10^{-2}
S_l : Cross section area of the link	m^2	1.95×10^{-5}
S_c : Cross section area of the clamp-part	m^2	8.09×10^{-4}
S_a : Cross section area of the actuator	m^2	1.58×10^{-5}
I_{zl} : Cross section area moment of inertia around z-axis of the link	m^4	2.75×10^{-12}
I_{zc} : Cross section area moment of inertia around z-axis of the clamp-part	m^4	3.06×10^{-8}
I_{za} : Cross section area moment of inertia around z-axis of the actuator	m^4	1.61×10^{-11}
E_l : Young's Modulus of the link	GPa	7.03×10^{1}
E_c : Young's Modulus of the clamp-part	GPa	7.00×10^{4}
E_a : Young's Modulus of the actuator	GPa	4.40×10^{1}
ρ_l : Density of the link	kg/m^3	2.68×10^{3}
ρ_c : Density of the clamp-part	kg/m^3	9.50×10^{2}
ρ_a : Density of the actuator	kg/m^3	3.33×10^{3}
α : Damping factor of the link	-	2.50×10^{-4}

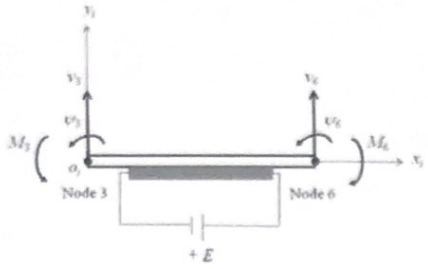

Fig.3. Modeling of the piezoelectric actuator

Furthermore, the voltage to generate the bending moments is proportional to the strain ε of the single-link due to the vibration. The relation can be expressed as follows

$$E = \pm \frac{1}{d_2} \varepsilon \tag{8}$$

Here d_2 is a constant quantity. Then, d_1 and d_2 will be determined by comparing the calculated results and experimental ones.

Computational codes were developed to perform dynamics simulation of the system based on the formulation that explained above. The validation was done using time history responses analysis of free vibration, natural frequencies using FFT (Fast Fourier Transform) processing, vibration modes and natural frequencies using eigenvalues-eigenvectors analysis and time history responses analysis due to the base excitation [1] – [4].

4 CONTROL SCHEME AND STRATEGIES

A control scheme to suppress the vibration of the single-link was designed using the piezoelectric actuator. It was done by adding bending moments generated by the piezoelectric actuator to the single-link. Therefore, the equation of motion of the system become

$$\boldsymbol{M}_n \ddot{\boldsymbol{\delta}}_n + \boldsymbol{C}_n \dot{\boldsymbol{\delta}}_n + \left[\boldsymbol{K}_n - \dot{\theta}^2(t) \boldsymbol{M}_n \right] \boldsymbol{\delta}_n = \ddot{\theta}(t) \boldsymbol{f}_n + \boldsymbol{u}_n(t) \tag{9}$$

Where the vector $\boldsymbol{u}_n(t)$ containing M_3 and M_6 is the control force generated by the actuator to the single-link.

To drive the actuator, two different control strategies namely P and AF controls have been designed and examined. Their performances were compared through calculations and experiments.

4.1 Proportional control

Based Substituting Eq. (8) to Eq. (7) gives

$$M_3, M_6 = \pm \frac{d_1}{d_2} \varepsilon \tag{10}$$

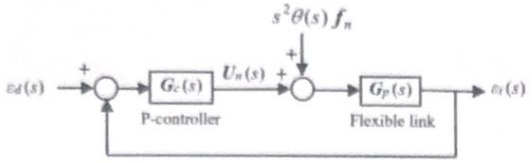

ε_d : Desired strain — ε_i : Measured strains at Node i
θ : Rotation angle of the motor — U_n : Applied bending moments

Fig.4. Block diagram of proportional control of the flexible link manipulator

Based on Eq. (10), the bending moments can be defined in s-domain as follows

$$\boldsymbol{U}_n(s) = \boldsymbol{G}_C(s)\left(\varepsilon_d(s) - \varepsilon_6(s)\right) \tag{11}$$

where ε_d and ε_6 denote the desired and measured strains at Node 6, respectively. The gain of P-controller can be written by a vector in s-domain as follows

$$\boldsymbol{G}_C(s) = \left\{0 \quad 0 \quad 0 \quad K_p \quad 0 \quad -K_p \quad 0 \quad \cdots \quad 0\right\}^T \tag{12}$$

Moreover, $\boldsymbol{G}_P(s)$ is transfer function of the n elements flexible link. A block diagram of the proportional control strategy for the single-link system is shown in Fig. 4.

4.2 Active-force control

Fig. 5 shows the block diagram of the AF control that is proposed in this research. In this strategy, vibration of the system is controlled by canceling bending moments acting at Nodes 3 and 6 due to the base excitation (excitation bending moments). The following steps are the way to estimate and cancel the excitation bending moments.

Firstly, the strain, ε_6 at Node 6 is measured to estimate the lateral deformation, v_6 at the Node 6. The relation between the strain and the lateral deformation considering the boundary conditions can be defined as follows

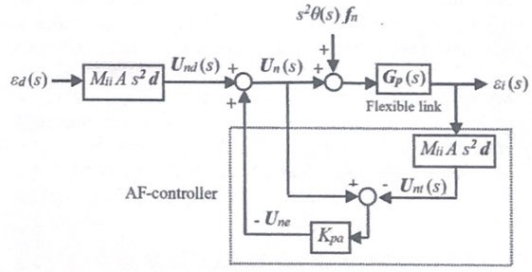

ε_d : Desired strain — ε_i : Measured strains at Node i
θ : Rotation angle of the motor — M_{li} : Component of mass matrix
A : Conversion from ε_i to v_i — $\boldsymbol{d}$: Position vector
U_{nd} : Desired bending moments — U_n : Applied bending moments
U_{ne} : Excitation bending moments — U_{nt} : Bending moments

Fig.5. Block diagram of active-force control of the flexible link manipulator

$$\frac{v_6}{\varepsilon_6} = -\frac{x^2(x-3l)}{6y(x-l)} = A \tag{13}$$

where l, x and y are the length of the link, the position of Node 6 in x and y directions, respectively.

Secondly, the actual force in the s-domain acting at Node 6 can be defined in the form of the Newton's equation of motion as follows

$$F_6(s) = M_{ii(i=11)}\, s^2\, v_6 \tag{14}$$

where $M_{ii(i=11)}$ is the component of the mass matrix corresponding to v_6.

Thirdly, the bending moments acting at Nodes 3 and 6 are estimated using the following equation

$$\boldsymbol{U}_{nl}(s) = \pm F_6(s)\boldsymbol{d} \tag{15}$$

The vector $\boldsymbol{d}$ that represents the position vector from the reference point to the position where the excitation force acting can be written as follows

$$\boldsymbol{d} = \{0 \;\; 0 \;\; 0 \;\; l_2 \;\; 0 \;\; l_2 \;\; 0 \;\; \cdots \;\; 0\}^T \tag{16}$$

Fourthly, based on Fig. 6, the excitation bending moments can be calculated as

$$\boldsymbol{U}_{ne}(s) = K_{pa}\{\boldsymbol{U}_{nl}(s) - \boldsymbol{U}_n(s)\} \tag{17}$$

where K_{pa} is the non-dimensional proportional gain of the proposed AF control.

Finally, the bending moments applying as a control force to control the vibration of the system can be calculated as follows

$$\boldsymbol{U}_n(s) = -\boldsymbol{U}_{ne}(s) + \boldsymbol{U}_{nd}(s) \tag{18}$$

where $\boldsymbol{U}_{nd}(s)$ is the desired bending moments which is zero. The negative of $\boldsymbol{U}_{ne}(s)$ indicates that the bending moments used to cancel the vibration of the system.

5 EXPERIMENT

5.1 Experimental set-up

In order to investigate the validity of the proposed control strategies, an experimental set-up was designed. The set-up is shown in Fig.6. The flexible link manipulator consists of the flexible aluminum beam, the clamp-part, the servo motor and the base. The flexible link was attached to the motor through the clamp-part. In the experiments, the motor was operated by an independent motion controller. A strain gage was bonded to the position of 0.11 m from the origin of the link.

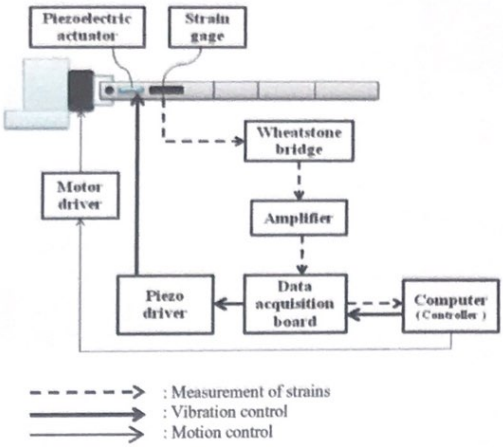

Fig.6. Schematics of measurement and control system [2]

The piezoelectric actuator was attached on one side of the flexible manipulator to provide the blocking force against vibrations. A Wheatstone bridge circuit was developed to measure the changes in resistance of the strain gage in the form of voltages. An amplifier circuit was designed to amplify the small output signal of the Wheatstone bridge.

Furthermore, a data acquisition board and a computer that have functionality of A/D (analog to digital) conversion, signal processing, control process and D/A (digital to analog) conversion were used. The data acquisition board connected to the computer through USB port. Finally, the controlled signals sent to a piezo driver to drive the piezoelectric actuator in its voltage range.

5.2 Experimental method

The rotation of the motor was set from 0 to $\pi/2$ radians (90 degrees) within 0.68 second. The outputs of strain gage were converted to voltages by the Wheatstone bridge and magnified by the amplifier. The noises that occur in the experiment were reduced by a 100 μF capacitor attached to the amplifier. The output voltages of the amplifier sent to the data acquisition board and the computer for control process.

Both of control strategies were implemented in the computer using the visual C++ program. The analog output voltages of the data acquisition board sent to the input channel of the piezo driver to generate the actuated signals for the piezoelectric actuator.

6 CALCULATED AND EXPERIMENTAL RESULTS

6.1 Calculated results

Time history responses of strains on the uncontrolled and controlled systems were calculated when the motor rotated by the angle of $\pi/2$ radians (90 degrees) within 0.68

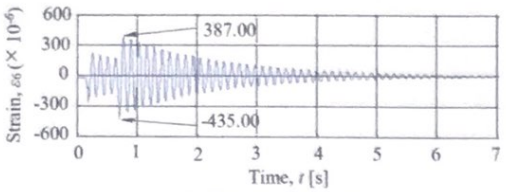

(a) Uncontrolled system

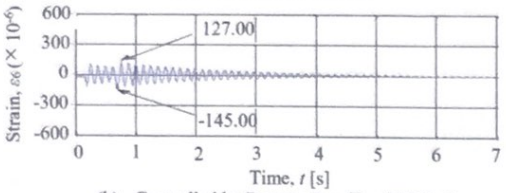

(b) Controlled by P-controller, K_p = 30 [Nm]

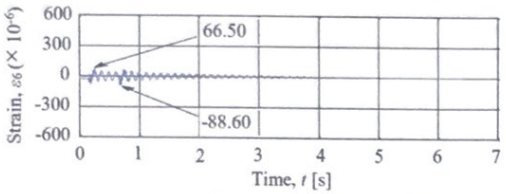

(c) Controlled by AF-controller, K_p = 0.4 [-]

Fig.7. Calculated time history responses of strains at Node 6 for uncontrolled and controlled system due to the base excitation

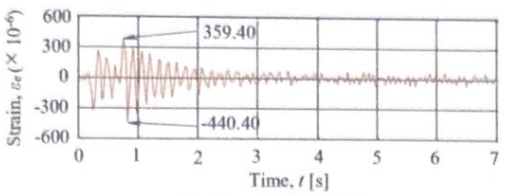

(a) Uncontrolled system

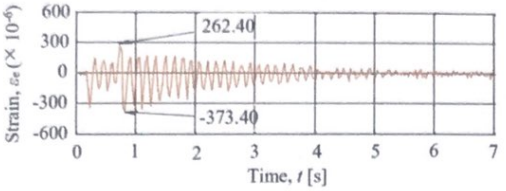

(b) Controlled by P-controller, K_p = 600 [-]

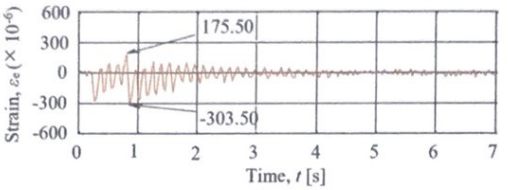

(c) Controlled by AF-controller, K_p = 125 [-]

Fig.8. Experimental time history responses of strains at 0.11 [m] from the link's origin for uncontrolled and controlled system due to the base excitation

seconds. Time history responses of strains on the controlled system were calculated for the model under three control strategies as shown in figures 7 and 8.

Examining several gains of the P and AF controllers leaded to K_p = 30 [Nm] and K_{pa} = 0.83as the better ones. Figure 9 shows the uncontrolled and controlled time history responses of strains at Node 6. The maximum and minimum strains of uncontrolled system in positive and negative sides were 387.00×10^{-6} and -435.00×10^{-6}, as shown in figure 9(a). By using P-controller they became 127.00×10^{-6} and -145.00×10^{-6}, as shown in figure 9(b). Moreover, by using AF-controller they became 66.50×10^{-6} and -88.60×10^{-6}, as shown in figure 9(c).

6.1 Experimental results

Experimental time history responses of the strains on the uncontrolled and controlled systems were measured when the motor rotated by the angle of $\pi/2$ radians (90 degrees) within 0.68 seconds. Experimental time history responses on the controlled system were measured under the control strategies as shown in figures 6 and 7.

Furthermore, the experimental active-force and proportional gains that are non-dimensional gains, K_p' and K_{pa} were examined. The examination of gains leaded to K_p' = 600 [-] and K_{pa}' = 125 [-], as the better ones. Figure 10 shows the experimental uncontrolled and controlled time history responses of strains at the same position in the calculations. The maximum and minimum strains of uncontrolled system in positive and negative sides were 359.40×10^{-6} and -440.40×10^{-6}, as shown in figure 10(a). By using P-controller they became 262.40×10^{-6} and -373.40×10^{-6}, as shown in figure 10(b). Moreover, by using AF-controller they became 175.50×10^{-6} and -303.50×10^{-6}, as shown in figure 10(c).

7 CONCLUSIONS

The equations of motion for the flexible single-link manipulator had been derived using the finite-element method. Computational codes had been developed in order to perform dynamic simulations of the system. Experimental and calculated results on time history responses, natural frequencies and vibration modes show the validities of the formulation, computational codes and modeling of the system. The proportional (P) and active-force (AF) controls strategies were designed to suppress the vibration of the system. Their performances were compared through the calculations and experiments. The calculated and experimental results show the superiority of the proposed AF control compared to the P one to suppress the vibration of the flexible single-link manipulator.

A flexible two-link manipulator is being prepared. The control scheme and strategies presented in this paper will be applied to the flexible two-link system.

REFERENCES

[1] A.K. Muhammad et al, "Computer Simulations on Vibration Control of a Flexible Single-link Manipulator Using Finite-element Method", *Proceeding of 19th International Symposium of Artificial Life and Robotics*, 2014, pp. 381 – 386.

[2] A.K. Muhammad et al, "Computer Simulations and Experiments on Vibration Control of a Flexible Link Manipulator Using a Piezoelectric Actuator", *Lecture Notes in Engineering and Computer Science: Proceeding of The International MultiConference of Engineers and Computer Scientists* 2014, IMECS 2014, 12 – 14 March, 2014, Hong Kong, pp. 262 – 267.

[3] A.K. Muhammad et al, "Comparisons Proportional-derivative and Active-force Controls on Vibration of a Flexible Single-link Manipulator Using Finite-element Method", *International Journal of Artificial Life and Robotic* Vol.19, 2014 (Accepted).

[4] A.K. Muhammad et al, "Computational Simulations on Vibration Control Scheme of a Flexible Single-link Manipulator", *Proceeding of Society of Instrument and Control Engineers (SICE) Shikoku, Japan*, 2013, pp. 199 – 203.